



## Biosynthesis and Characterization of Silver Nanoparticles Produced by Plant Extracts and Its Antimicrobial Activity

Marwa A. Samy<sup>1,2</sup>, Moustafa A. Abbassy<sup>1</sup>, Elsayed E. Hafez<sup>2</sup>, Entsar I. Rabea<sup>1\*</sup> and Dalia G. Aseel<sup>2</sup>

<sup>1</sup>Department of Plant Protection, Faculty of Agriculture, Damanhur University, Damanhur, 22516, Egypt.

<sup>2</sup>Department of Plant Protection and Bio-Molecular Diagnosis, Arid Lands Cultivation Research Institute, City of Scientific Research and Technological Applications, New Borg Elarab, 21934, Alexandria, Egypt.

### Authors' contributions

This work was carried out in collaboration between all authors. Authors MAA, EEH, MAS designed the study, performed the statistical analysis, wrote the protocol and wrote the first draft of the manuscript. Authors EIR and DGA managed the analyses of the study and the literature searches. All authors read and approved the final manuscript.

### Article Information

DOI: 10.9734/SAJRM/2019/v3i130077

#### Editor(s):

(1) Dr. Obafemi Yemisi Dorcas, Assistant Lecturer, Department of biological Sciences, Covenant University, Ota, Ogun State, Nigeria.

(2) Dr. Chamari Hettiarachchi, Senior Lecturer, Department of Chemistry, University of Colombo, Sri Lanka.

#### Reviewers:

(1) Nguyen Thi Hieu Trang, Vietnam.

(2) Ajoy Kumer, European University of Bangladesh, Bangladesh.

(3) Tahmina Monowar, AIMST University, Malaysia.

Complete Peer review History: <http://www.sdiarticle3.com/review-history/46186>

Original Research Article

Received 30 October 2018  
Accepted 03 February 2019  
Published 13 March 2019

### ABSTRACT

*Solanum tuberosum* is the fourth most challenging plant in Egypt, affected by several fungi, viral and bacterial diseases. Bacterial and fungal isolates (Brown rot disease (*Ralstonia solaniserum*), soft root disease (*Pectobacterium carotovora*) and dry rot disease (*Fusarium oxisporum*) were collected. The green extracts of silver nanoparticles were prepared by means of aqueous extracts of three wild plants, *Physalis peruviana* (leaves, red and green fruits) (N1, N2 and N3), *Solanum nigrum* (fruit) (N4) and *Moringa oliefera* (leaves) (N5). SEM, TEM, FT-IR and X-RD obtained the characterization of the biosynthesis of silver nanoparticles. The results indicated that nanoparticles

\*Corresponding author: Email: entsar\_ibrahim@yahoo.com;

were spherical, smooth and the sizes varied between 12 and 33 nm. The activity of the nanoparticle formulations was tested against the bacterial isolates using agar diffusion method and one fungus using mycelial growth method. The results also elucidated that N5 formulation showed a significantly potent antibacterial activity against *R. solanacearum*. However, N1 formulation was the highest active one against *P. carotovra*. In addition, the antifungal activity indicated that N1 had the highest effect ( $EC_{50} = 687.03$  mg/L) followed by N3 ( $EC_{50} = 981.61$  mg/L) against *F. oxysporium*. Nanoparticles synthesized by wild plants could be used as safe alternatives to harmful microbicides.

**Keywords:** Biosynthesis; silver nanoparticles; *physalis peruviana*; *Solanum nigrum*; *Moringa oliefera*; plant extract; antifungal; antibacterial; SEM; TEM; FT-IR; XRD.

## 1. INTRODUCTION

*Solanum tuberosum* (family Solanaceae) is a worldwide-cultivated tuber-bearing plant, which is the fourth main food crop in the world after rice (*Oryza sativa*), maize (*Zea mays*) and wheat (*Triticum aestivum*), in terms of both area cultivated and total production [1,2]. Potato does not need exceptional growth circumstances; it has been for a long time a most important field crop in temperate regions, and progressively in warmer areas [3]. It is presently the second greatest significant vegetable crop after tomatoes in Egypt, and Egypt is one of Africa's prime potato producers and exporters. Potato is vulnerable to a numeral of diseases, enclosing late blight triggered by *Phytophthora infestans*, numerous viruses and bacterial wilt caused by *Ralstonia solanacearum*. Bacteria and fungi are played a primary character in the harvest losses, particularly *Erwinia* the causal agent of soft rot in potato [4] and *Alternaria spp* the causal agent of early blight of potato [5]. *Ralstonia solanacearum*, the causative agent of bacterial wilt in potatoes, is soilborne and can persist in soil for a long time in infected host plant debris or by colonizing potato volunteer plants, alternative hosts or even non-host plants [6]. To infect a plant effectively, the pathogen first has to be capable to penetrate and colonize host tissues and overcome active plant defense responses to encourage the set of actions finally that leads to disease symptoms. Furthermore, *Pectobacterium carotovra* is a gram-negative phytopathogenic bacterium, which attack carrots, cucumber, onions, potatoes and tomatoes. It produced black leg (soft rot) to these plants through farming, transportation and storage [7]. *Pectobacterium* produced damage of the cell wall of the plants then cause death of the plants. Fusarium wilt diseases are accountable for imperative harvest damages on several crops. *Fusarium oxysporum* causes dry rot, stem-end rot and wilt of potatoes. Fusarium dry rot is mainly a post-harvest disease

and can turn into a foremost problem when infected stored potatoes. Chemical control of potato brown rot with currently existing crop protectants is not effective [8]. Improvement of additional effective chemical control techniques is not fortified owing to the universal awareness about adverse impacts of synthetic crop protectants on human health and the environment; this has led to the phasing out of an increasing quantity of crop protectants. Consequently, there is a perfect necessity to improve alternative practical, harmless and effective managing approaches that can condense the time that no host plants can be grown. Plant extracts of many higher plants have been described to display antibacterial and antifungal properties under laboratory trails [9,10]. Plant metabolites and plant-based pesticides seem to be one of the improved alternatives, as they are known to have minimal environmental impact and hazard to consumers in contrast to the synthetic pesticides [11]. Nanotechnology has been used widespread in plant pathogens and the application of nanoparticles become essential in the managing of plant diseases [12]. Silver nanoparticles exhausting plant extracts are a significant distinction chemical and biosynthetic using gold, platinum and silver in the synthesized of nanoparticles [13]. Therefore, the current study goals to synthesize silver nanoparticles by a green biological route, using an extract derived from *Physalis peruviana* (leaves, red and green fruits), *Solanum nigrum* (fruit) and *Moringa oliefera* (leaves). Characterization of the synthesized nanoparticles achieved using scanning electron microscope (SEM), transmission electron microscope (TEM), X-ray diffraction (XRD) and Fourier transform infrared spectroscopy (FT-IR) analysis. Besides, their antimicrobial activity against representatives of plant pathogenic bacteria (*Pectobacterium carotovra* and *Ralstonia solaniserum*) and fungus (*Fusarium oxysporium*) was investigated.

## 2. MATERIALS AND METHODS

### 2.1 Cultures and Growth Conditions

The potato plants were grown at two localities in Abo-Homous and Borg-Elarb, El-Behera and Alexandria Governorates, respectively, Egypt during the growing season 2016. The bacteria were isolated from infected potato tubers and purified on Luria Bertani medium (LB) [14], and incubated for 24 hours at 30°C. In addition, the fungi was grown on Potato dextrose agar (PDA) and Kelman's TZC media [15], then incubated at 28°C for 7 days. The microbes (bacteria and fungi) were identified using different methods including microscopically extension and molecular identification.

### 2.2 Pathogenicity Test

According to Zhang et al. [16] with some modification, healthy potato tubers selected and washed carefully in water. Tubers dipped in ethanol 70% for 5 min and washed in distilled water. Sterilized tuber was inoculated by syringe in plates containing a piece of sterile cotton saturated with water. The suspension concentration of bacteria and fungi were  $10^8$  and  $10^6$  CFU/mL, respectively. Control tubers were inoculated by distilled water and incubated at the same conditions.

### 2.3 Preparation of the Plant Extracts

Three medicinal plants, *P. peruviana* (leaves, red and green fruits), *S. nigrum* (fruit) and *M. oleifera* (leaves) were selected from Abo-Homous and Borg-Elarb, El-Behera and Alexandria Governorates, respectively, Egypt. Fresh and healthy leaves and fruits were collected locally and rinsed thoroughly first with tap water followed by distilled water to remove all the dust and unwanted visible particles, cut into small pieces and dried at room temperature. About 10 g of these finely incised leaves of each plant type were weighed separately, 100 mL distilled water was added and boiled for about 20 min. The extracts were then filtered thrice to get clear solutions, which were then, refrigerated (4°C) for further experiments [17].

### 2.4 Green Synthesis of Silver Nanoparticles Formulations

Plant extract was added to aqueous solution (10 mM) of silver nitrate ( $\text{AgNO}_3$ ) in dark flask with shaking at 250 rpm and the changes in the color was observed. The reduction of Ag solution was

subjected to UV- Visible spectrophotometer at 540 nm (Beckman, model Du 540), and the reaction stopped when the value of optical density was decreased. The solution was centrifuged at 12000 rpm for 30 min, the supernatant was discard and the pellet washed 3 times by sterile water. The pellet was dried at 50°C and then dissolved in sterile water [17].

### 2.5 Characterization of Silver Nanoparticles Formulations

#### 2.5.1 Scanning electron microscopy (SEM)

Scanning electron microscopy (SEM) is a method for high-resolution imaging of surfaces. SEM analysis was done by using a JEOL JSM-5410 (Japan) electron microscope with a W-source and operating at 80 kV. Sample was prepared on a glass slide (1 × 1 cm) after washing it with ethanol. A tiny drop of nanoparticles was spreaded evenly over glass slide and allowed to air dry. In order to make it conductive, gold coating with Jeol Quick Auto Coater was performed (JFC-1500). The NPs were then subjected to SEM analysis under ambient conditions.

#### 2.5.2 Transmission electron microscopy (TEM)

Morphology of the nanoparticles usually determined by transmission electron microscopy (TEM). A combination of bright-field imaging at increasing magnification and of diffraction modes use to reveal the form and size of the nanoparticles. To perform the TEM observations, the nanoparticles formulation dilute with water (1/100). A drop of the diluted nanoparticles directly deposited on the film grid and observed after dry.

#### 2.5.3 Fourier transform infrared spectroscopy (FT-IR)

FTIR spectra of nanoparticles were taken with potassium bromide pellets on a Thermo Nicolet AVATAR 300 FTIR spectrometer in the range 400-4000  $\text{Cm}^{-1}$ .

#### 2.5.4 X-ray diffraction analysis (XRD)

X-ray powder diffraction patterns of nanoparticles were obtained by a D/max-rA diffractometer. The X-ray source was CuK radiation (40 kV, 80 mA). Samples were scanned at a scanning rate of 4°/min.

## 2.6 Assessment of Antimicrobial Assay

### 2.6.1 Antibacterial activity of nanoparticles formulations

The antibacterial activity of the nanoparticles was evaluated against *P. carotovra* and *R. solaniserum* by the agar diffusion method with LB agar media. A 20 mL of LB agar media was poured into sterilized petri dishes and the plates were leaved for solidification then bacterial suspension of the two tested bacteria was streaked. The paper discs of 6 mm size were saturated with 20  $\mu$ L of silver nanoparticles solutions (100, 200, 400 and 600 mg/L) or Doxycycline (30  $\mu$ g) as standard antibacterial agent and plated on the surface of each plates at equivalent distance with control. Bacteria was stand by 30 min, then incubated at 30°C for 24 h and the formed inhibition zone was measured and three replicates were used [18].

### 2.6.2 Antifungal activity of nanoparticles formulations

The antifungal activity was tested using mycelia radial growth technique [19]. The compounds were dissolved and serial concentrations ranged from 1000 to 3000 mg/L were tested. Standard fungicide, gold plus was used at 0.25, 0.5 and 1.0 fold of field application (200 g/100 L). The aliquots (quantity) of the stock solutions were added to the PDA medium, and then transferred to Petri dishes. After solidification, the mixtures were inoculated with a 5 mm in diameter mycelium fungi at the center of Petri dishes and these were incubated in the dark at  $27 \pm 2^\circ\text{C}$ . Fungal growth was measured when the control had grown to the edge of the plate. The inhibition of fungal growth was calculated as the percentage of inhibition of radial growth compared to the control. The effective concentration that inhibits 50% of mycelial growth ( $EC_{50}$ ) for each compound was estimated by probit analysis [20] using SPSS 21.0 software.

## 2.7 Molecular Identification of Obtained Isolates Using Specific PCR, Sequencing and Phylogenetic Analysis

DNA was isolated from the two bacterial isolates and the fungus isolate using QIAgene DNA extraction kit according to the manufacture procedures (QIAgene, Germany). PCR amplification for the bacteria was performed

using the 16S rRNA primers (forward; AGAGTTTGATCCTGGCTCAG and reverse; AAGGAGGTGATGCAGCC) according to Weisbrug et al. [21]. On the other hand, the fungus DNA was subjected to PCR amplification using ITS specific primers (ITS1; TCCGTAGGTGAACCTGCGG and ITS4; TCCTCCGCTTATTGATATG) according to White et al. [22]. The 25  $\mu$ L PCR reaction components were; 12.5  $\mu$ L master mix (Applied Biotechnology, Egypt), 1  $\mu$ L DNA (30 ng), 1  $\mu$ L for each primer (10 p mol /  $\mu$ L) and the volume completed up to 25  $\mu$ L with sterile  $\text{H}_2\text{O}$ . The PCR program was applied as follow; initial denaturation at 95°C for 2 min; 34 cycles of 94°C for 1 min; annealing at 55°C for 1 min; extension at 72°C for 1 min and a final extension step at 72°C for 5 min; A 5  $\mu$ L of PCR products were separated on 2% (w/v) agarose gel electrophoresis in 0.5x TBE buffer. The molecular weight of band was estimated using DNA marker (marker size). Finally, the gel was photographed using gel documentation system. PCR products were purified using PCR clean up column kit (Maxim biotech INC, USA). The purified PCR products were subjected to DNA sequencing using the forward primer of 16S rRNA and ITS (Sigma company, Korea). The DNA nucleotide sequences were alignment using BLASTn (<http://www.ncbi.nlm.gov/BLAST>) and then the clean sequences was submitted to Gene Bank. Phylogenetic tree was constructed using Mega 4 program, to examine the origin of the obtained microbial strains [23].

## 2.8 Statistical Analysis

Statistical analysis was performed using SPSS 21.0 software (Statistical Package for Social Sciences, USA). All experiments were repeated at least 3 times. The data were expressed as the mean  $\pm$  standard error (SE). The log dose-response curves allowed determination of the  $EC_{50}$  values for the fungal bioassay according to the probit analysis [20]. The 95% confidence limits for the range of  $EC_{50}$  values were determined by the least-square regression analysis of the relative growth rate (% control) against the logarithm of the compound concentration.

## 3. RESULTS AND DISCUSSION

### 3.1 Pathogenicity Test

Many different bacteria and fungi were successfully isolated from collected potato tuber,

they include; *P. carotovra*, *R. solanacearum* and *F. oxysporum*, all of which were implicated as pathogens when tested on healthy tubers. The bacterial isolate showed high capability for infection the healthy potato tubers. *P. carotovra* causes soft rot disease symptoms in the inoculated healthy potato tubers after 4-5 days post inoculation. The appeared symptoms were; chlorosis, wilting, tuber rot, blackleg and haulm desiccation. These results are in agreement with those obtained by Motyka et al. [24] and Onkendi and Moleleki, [25]. While, healthy potato tuber inoculated with *R. solanacearum* was showed the wilt disease symptoms; vascular browning, dark brown streaks and grey-white bacterial ooze was observed on tuber surfaces. Moreover, the *F. oxysporium* was isolated and used in inoculation of the healthy tubers and it was observed that the isolate succeeded to cause dry rot disease for the tubers after 7 days. The observed symptoms were; dry rot, sunken, wrinkled and a white mold was visible on tuber surfaces (Fig. 1).

### 3.2 Molecular Identification of the Obtained Isolates

Approximately 1500 bp region of the 16SrRNA gene was amplified for *P. carotovra* and *R. solanacearum*, while, PCR product of ITS gene amplified 550 bp for *F. oxysporium* (Fig. 2) using universal primers. The DNA sequence results revealed that the examined two bacteria and one isolate of fungi. The phylogentic tree constructed based on the obtained DNA sequence revealed that *P. carotovra* contained of two cluster; cluster one was divided into two sub cluster, sub cluster one was divided into two group, group one divided to two sub group which contain *P. carotovra* that similar with investigated isolate with different percentage. *R. solanacearum* had phylogenetic tree contained two cluster; cluster one contain *R. solanacearum* isolate whereas cluster two consist two sub cluster that divided into two group which divided into two sub group that contain different strains of *R. solanacearum*. The phylogenetic tree of *F. oxysporium* contains two cluster; cluster one divided to two sub cluster, sub cluster one contain to two group that divided into two sub group which contain strains of *F. oxysporium*. While cluster two contain two sub cluster, cluster two divided into two group, group two contain two sub group while sub group two contain detected isolate of Fusarium as shown in Fig. 3.

### 3.3 Green Synthesis of Silver Nanoparticles Using Plant Extracts

The synthesized nanoparticles using the five different aqueous plant extracts; *M. olifera* (leaves) *S. nigrum* (fruits) and *P. peruviana* (leaves, red and green fruits) were obtained after incubation period lasts for 24h. It was observed that the solution color changed from yellow to dark brown within the first 10 hrs. Silver nanoparticles exhibit yellowish brown color in aqueous solution due to excitation of surface plasmon vibrations in silver nanoparticles. Thus, plant extracts act as reducing agents as well as capping agents.

The papaya fruit extract was mixed in the aqueous solution of the silver ion complex; it started to change the color from watery to yellowish brown due to reduction of silver ion, which indicated formation of silver nanoparticles [26]. UV-Vis spectroscopy could be used to examine size- and shape-controlled nanoparticles in aqueous suspensions. Five plant leaf extracts (Pine, Persimmon, Ginkgo, Magnolia and Platanus) were used and compared for their extracellular synthesis of silver nanoparticles [27]. Stable silver nanoparticles were formed by treating aqueous solution of  $\text{AgNO}_3$  with the plant leaf extracts as reducing agent of  $\text{Ag}^+$  to  $\text{Ag}^0$ . Magnolia leaf broth was the best reducing agent in terms of synthesis rate and conversion to silver nanoparticles. The average particle size ranged from 15 to 500 nm. Silver nanoparticles were rapidly synthesized using leaf extract of *Acalypha indica* and the formation of nanoparticles was observed within 30 min with the size of 20–30 nm [28]. Ali et al. [29] showed that the leaf extract of menthol is very good bioreductant for the synthesis of silver nanoparticles and synthesized nanoparticles were found to be spherical in shape with 90 nm.

### 3.4 Characterization of Silver Nanoparticles Formulations

The obtained silver nanoparticles was subjected to different characterization methods; SEM, TEM, XRD and FT-IR. From the SEM and TEM micrograph of AgNPs, different extracts produce different size and different crystals, which occurs different effective of the activity of nanoparticles on organisms (Fig. 4). FT-IR results revealed that the obtained particles are silver nanoparticles when compared with the standard nanosilver profile (Fig. 5). It was noticed that extract which

produced silver nanoparticles in the range of 12-33 nm, and detected the function group which coated on the surface of particles by X-RD and FT-IR.

The biosynthesised silver nanoparticles by using papaya fruit extract was confirmed by XRD and SEM [26]. The characteristic peaks observed in the XRD image showed in (Fig. 6) three intense peaks in the whole spectrum of  $2\theta$  value ranging from 10 to 80. The XRD pattern average size of the particles synthesized was 15 nm with size

range 10 to 50 nm with cubic and hexagonal shape. The SEM image showing the high-density silver nanoparticles synthesized by the papaya extract further confirmed the development of silver nanostructures.

FT-IR analysis was used for the characterization of the extract and the resulting nanoparticles [30]. The peaks near  $3450\text{ cm}^{-1}$  and near  $2933\text{ cm}^{-1}$  were assigned to O-H stretching and aldehydic C-H stretching, respectively. The weaker band at  $1643\text{ cm}^{-1}$  corresponds

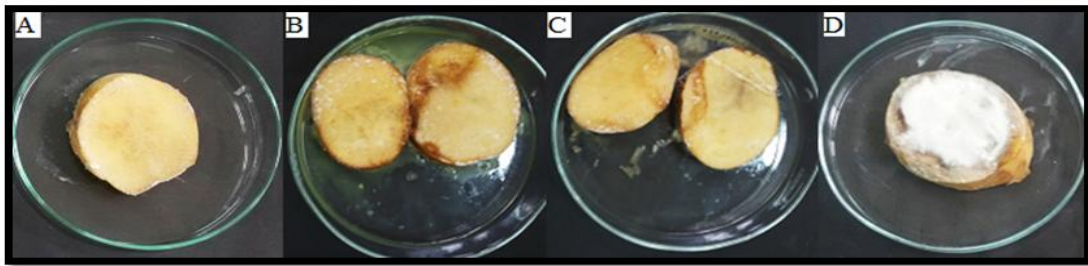


Fig. 1. Pathogenicity test of the potato tubers. Tuber control (A); tuber infected with *P. carotovra* (B); tuber infected with *R. solanacearum* (C) and tuber infected with *F. oxysporium* (D)

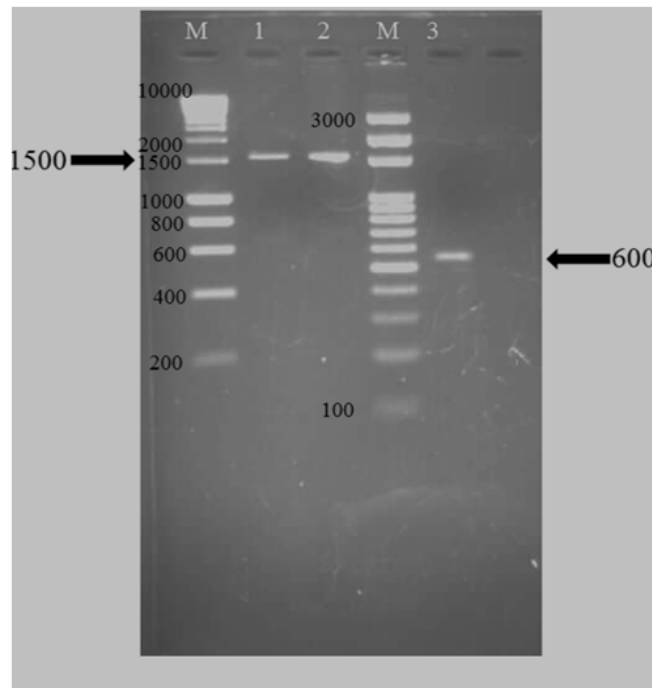
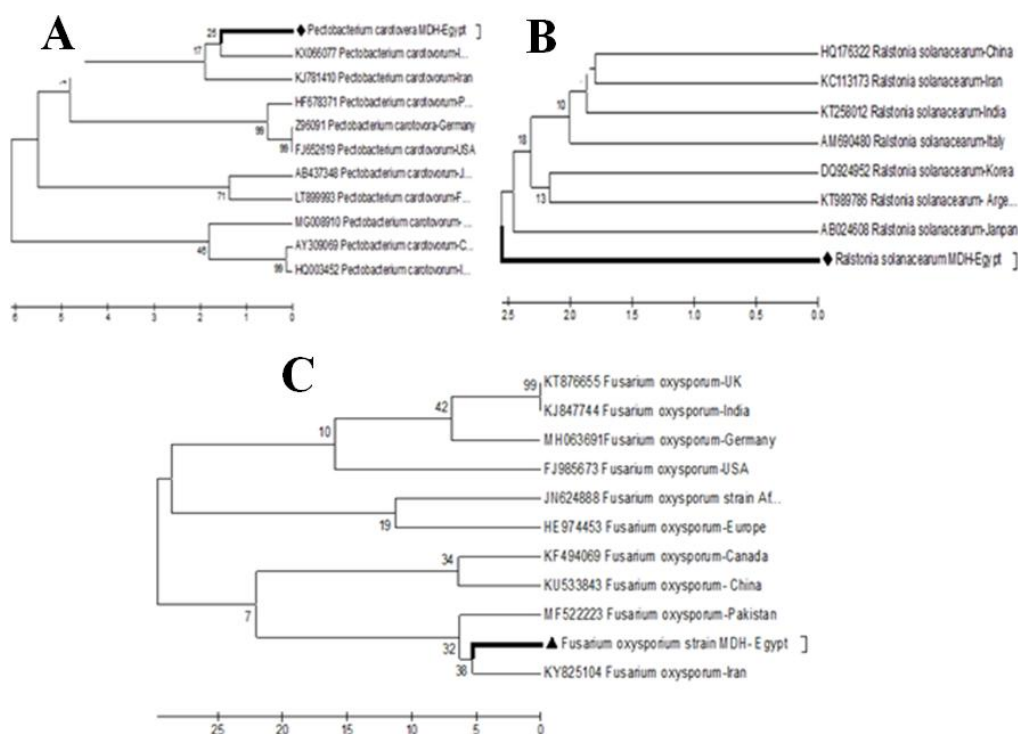


Fig. 2. PCR products of 16s RNA gene for both two bacterial isolates and ITS gene of fungi, respectively. M, 10000 Kbp DNA marker; Lane 1, *P. carotovra*; Lane 2, *R. solanacearum*; M, 3000 Kbp DNA marker; *F. oxysporium*



**Fig. 3. Phylogenetic tree of 16s RNA and ITS genes: *P. carotovra* (A); *R. solanacearum* (B) and *F. oxysporium* (C). Based on the DNA nucleotide sequencing and comparing with the other species listed in the Gene Bank**

to amide I, arising due to carbonyl stretch in proteins. The peak at  $1031\text{ cm}^{-1}$  corresponds to C–N stretching vibrations of the amine. IR spectroscopic study confirmed that the carbonyl group from amino acid residues and proteins has the stronger ability to bind metal indicating that the proteins could possibly form a layer covering the metal nanoparticles (i.e., capping of silver nanoparticles) to prevent agglomeration and thereby stabilize the medium. This suggests that the biological molecules could possibly perform dual functions of formation and stabilization of silver nanoparticles in the aqueous medium.

FTIR analysis was used for the characterization of the silver nanoparticles using *Garcinia mangostana* leaf extract [31]. Absorbance bands were observed at  $1619, 1522, 1340, 1160\text{ cm}^{-1}$ . These absorbance bands are known to be associated with the stretching vibrations for C–C– [(in-ring) aromatic], C–O–C (ethers) and C–O (–C–OH). In particular, the  $1160\text{ cm}^{-1}$  band arises most probably from the C–O of aromatic-OH group (such as hydroxyflavones and hydroxyxanthones). The total disappearance of this band after the bioreduction may be due to the fact that the polyols are mainly responsible

for the reduction of Ag ions, whereby they themselves get oxidized to unsaturated carbonyl groups leading to a broad peak at  $1660\text{ cm}^{-1}$  (for reduction of Ag) [26].

### 3.5 Antibacterial Activity of Silver Nanoparticles Formulations

The *in vitro* antibacterial activity of silver nanoparticles formulations against *R. solanacearum* and *P. carotovra* is presented in Table 1 using the agar diffusion method. The measured zone of inhibition of the silver nanoparticles formulations showed significantly different inhibitory effects. The results demonstrated that all formulations showed good inhibition (Inhibition (%) ranged from 20.56 to 29.26 %) against the tested bacteria and the inhibitory effects were concentrations dependent. For the five silver nanoparticles formulations, N5 formulation exerted significantly potent antibacterial activity against *R. solanacearum*. Followed by N4 in the descending order. However, N1 formulation was the lowest active as showed in Fig. 7. Against *P. carotovra*, N1 formulation exerted significantly potent antibacterial activity. Followed by N5 in the



descending order. However, N4 formulation was the lowest active as showed in Fig. 7. When we consider the susceptibility of the microorganisms, another point deserves attention; it can be noticed that bacterium of *P. carotovra* was more susceptible than *R. solanacearum* to all formulations (Table 1 and Fig. 7). It appears that the antibacterial activity of the silver nanoparticles formulations increased with increase in surface-to-volume ratio, due to the decrease in size of nanoparticles.

Antibacterial effects of Ag nanoparticles obeyed a dual action mechanism of antibacterial activity, i.e., the bactericidal effect of  $Ag^+$  and membrane-disrupting effect of the polymer subunits. The

antibacterial activities of Ag nanoparticles,  $Ag^+$  ions were blocked by thiolcontaining agents. Silver was also known to cause pits in bacterial cell walls, leading to an increased cell-membrane permeability and cell death [32]. The antibacterial activity of synthesized silver nanoparticles using leaf extract of *Acalypha indica* showed effective inhibitory activity against water borne pathogens, *Escherichia coli* and *Vibrio cholera* [28]. Silver nanoparticles 10 g/ml were recorded as the minimal inhibitory concentration (MIC) against *E. coli* and *V. cholerae*. Alteration in membrane permeability and respiration of the silver nanoparticle treated bacterial cells were evident from the activity of silver nanoparticles.

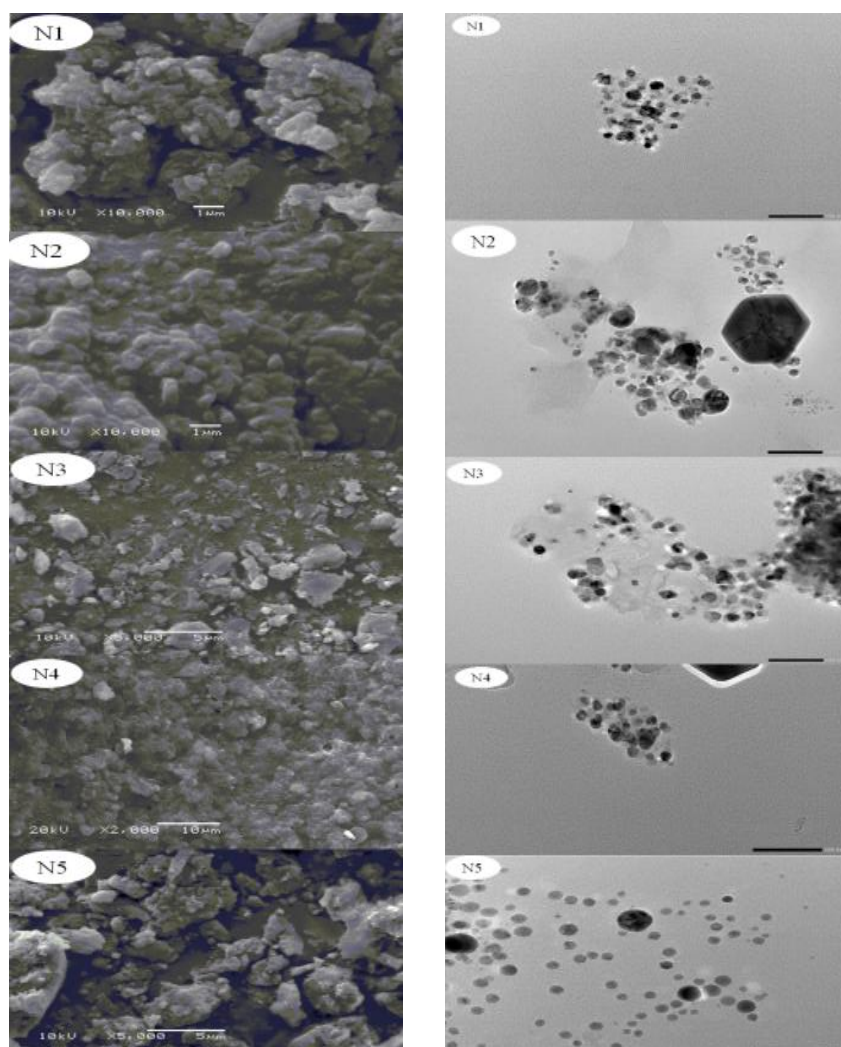


**Fig. 4. SEM (right) and TEM (left) of silver nanoparticles formulations, N1 to N5. The SEM was performed on a JEOL JSM-1200EX II scanning electron microscope operating at an acceleration voltage of 80.0 kV with 20  $\mu$ m aperture**



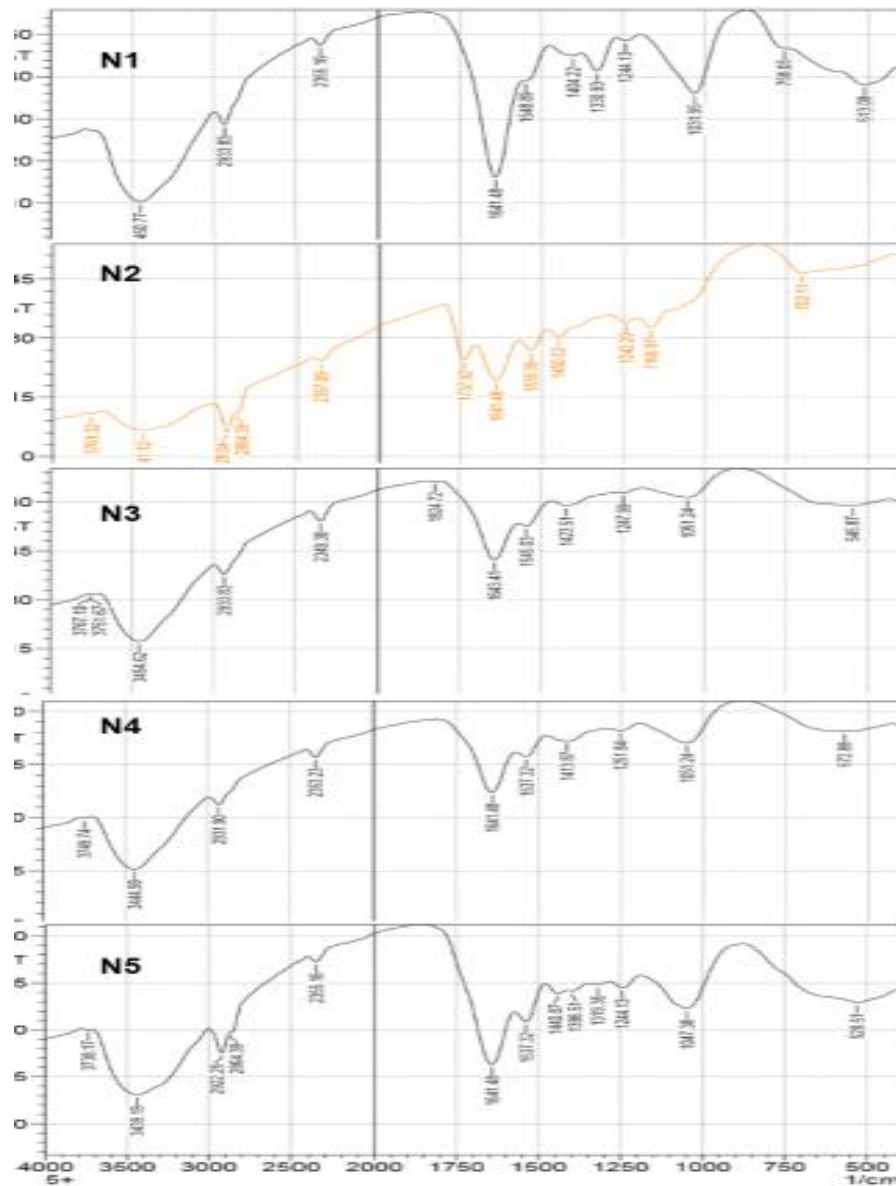


Fig. 5. The FT-IR spectra of the five biosynthesized silver nanoparticles: *S. nigrum* (N1); *P. peruviana* Red (N2); Leave *P. peruviana* (N3); Green *P. peruviana* (N4); *M. oliefera* (N5)

### 3.6 Antifungal Activity of Silver Nanoparticles Synthesized with Plant Extracts

The *in vitro* antifungal activity of silver nanoparticles formulations against the plant pathogenic fungus *F. oxysporum* is presented in Table 2 and the results are expressed as EC<sub>50</sub>. Most of the tested compounds showed inhibitory effect against tested fungus. For the five silver nanoparticles formulations, N1 formulation

exerted significantly potent antifungal activity with EC<sub>50</sub> of 687.03 mg/L against *F. oxysporum*. Followed by N3 in the descending order with EC<sub>50</sub> of 981.61 mg/L. However, N2 formulation was the lowest active (EC<sub>50</sub> = 1474.86 mg/L against tested fungus as showed in Fig. 8. Standard fungicide, Ridomil gold showed the highest fungicidal activity (EC<sub>50</sub> = 204.02 mg/L). From statistical analysis, there is no significant difference between standard fungicide and N1 formulation (see Table 2).

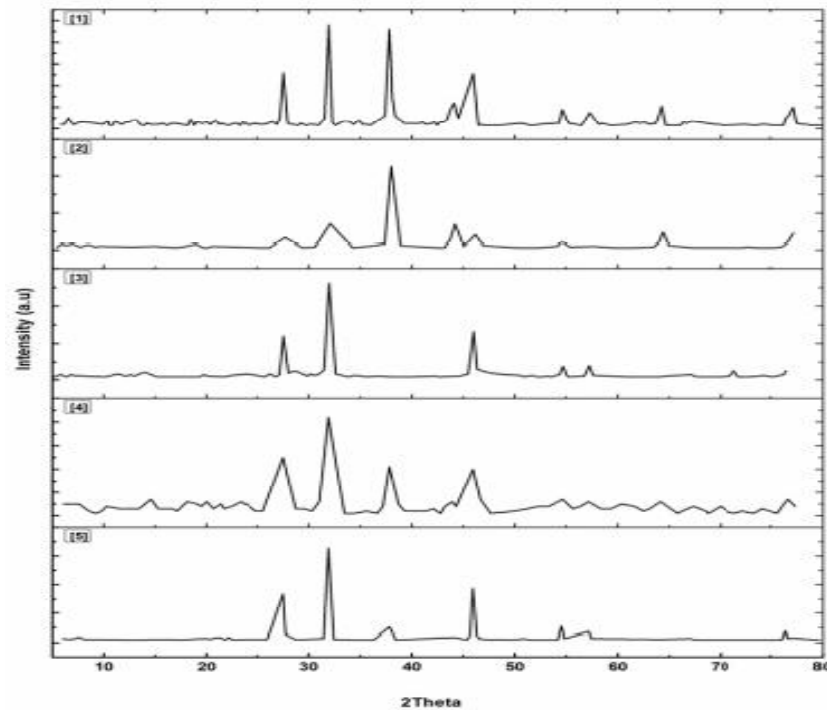
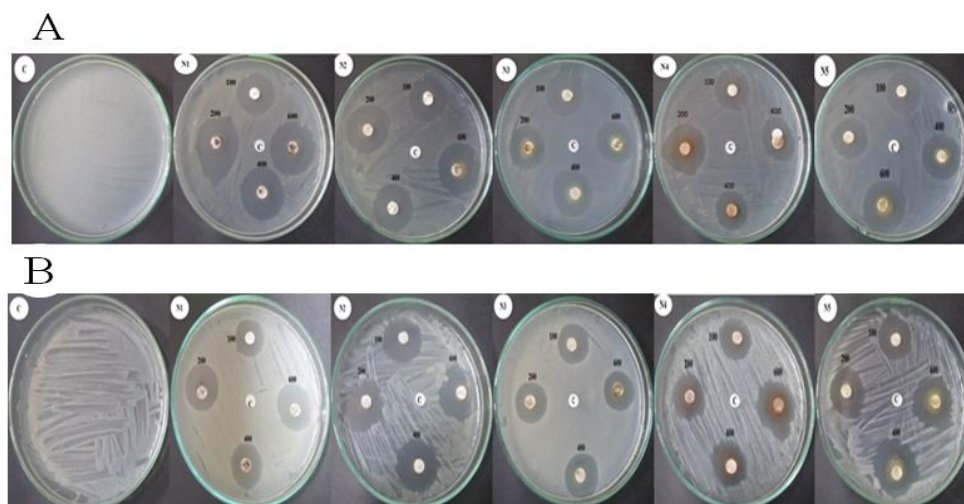


Fig. 6. The XRD analysis of the five biosynthesized silver nanoparticles: *S. nigrum* (N1); *P. peruviana* Red (N2); Leave *P. peruviana* (N3); Green *P. peruviana* (N4); *M. oliefera* (N5)

Table 1. The *in vitro* antibacterial activity of biosynthesized silver nanoparticles against *R. solanacearum* and *P. carotovra* by the agar diffusion method

Formulations	Conc. (mg/L)	Inhibition (%)	
		<i>R. solanacearum</i>	<i>P. carotovra</i>
N1	100	20.95 ± 1.39	23.70 ± 0.64
	200	21.48 ± 0.64	24.81 ± 1.70
	400	21.48 ± 2.24	27.04 ± 1.70
	600	22.22 ± 1.46	29.26 ± 0.64
N2	100	20.56 ± 1.11	21.07 ± 1.11
	200	23.04 ± 1.79	23.37 ± 1.89
	400	23.14 ± 2.62	25.9 ± 2.79
	600	24.63 ± 2.50	26.26 ± 1.45
N3	100	22.04 ± 0.32	23.70 ± 1.69
	200	22.96 ± 1.69	24.07 ± 1.89
	400	23.15 ± 1.15	25.00 ± 0.56
	600	23.26 ± 1.67	25.22 ± 0.91
N4	100	20.74 ± 2.56	16.85 ± 6.62
	200	21.85 ± 2.56	22.22 ± 3.33
	400	22.04 ± 4.01	22.59 ± 0.64
	600	25.00 ± 1.11	23.89 ± 2.00
N5	100	22.41 ± 0.32	21.85 ± 0.84
	200	26.30 ± 2.74	23.15 ± 1.60
	400	26.67 ± 1.11	26.67 ± 1.11
	600	27.04 ± 0.64	28.52 ± 2.31
<b>Doxycycline</b>	30	12.77 ± 0.40	22.89 ± 0.99

Green *P. peruviana* (N1); Red *P. peruviana* (N2); leaves of *P. peruviana* (N3); *S. nigrum* (N4) and *M. oliefera* (N5)



**Fig. 7.** The *in vitro* antibacterial activity of silver nanoparticles formulations against *P. carotovra* (A) and *R. solanacearum* (B) by the agar diffusion method with different concentrations (0, 100, 200, 400 and 600 mg/L, respectively). Green *P. peruviana* (N1); Red *P. peruviana* (N2); leaves of *P. peruviana* (N3); *S. nigrum* (N4) and *M. oleifera* (N5)

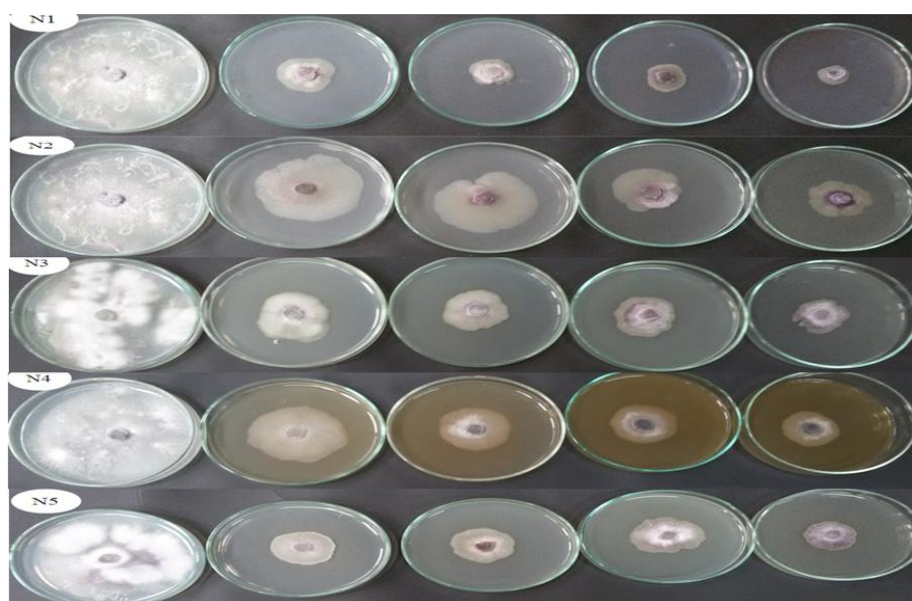


**Fig. 8.** The antifungal activity of the silver nanoparticles formulations (from left to right, 0, 1200, 1600, 2000 and 2400 mg/L, respectively) against *F. oxysporium*. Green *P. peruviana* (N1); Red *P. peruviana* (N2); leaves of *P. peruviana* (N3); *S. nigrum* (N4) and *M. oleifera* (N5)

Different concentrations of biosynthesized silver nanoparticles were tested to know the inhibitory effect of fungal plant pathogens namely *Alternaria alternata*, *Sclerotinia sclerotiorum*, *Macrophomina phaseolina*, *Rhizoctonia solani*, *Botrytis cinerea* and *Curvularia lunata*. Remarkably, 15 mg concentration of silver nanoparticles showed excellent inhibitory activity against all the tested pathogens [33]. Narayanan

and Park, [34] demonstrated the synthesis of silver nanoparticles using turnip leaf extract and its interaction with wood-degrading fungal pathogens, *Gloeophyllum abietinum*, *G. trabeum*, *Chaetomium globosum*, and *Phanerochaete sordida*. The synthesized silver nanoparticles showed broad-spectrum antifungal activity against wood-degrading fungi by inhibiting growth.

**Table 2. The *in vitro* antifungal activity of biosynthesized silver nanoparticles against *F. oxysporium* by mycelia radial growth technique**

Formulations	EC <sub>50</sub> <sup>a</sup> (mg/L)	95% confidence limits		Slope <sup>b</sup> ± SE	Intercept <sup>c</sup> ± SE	(χ <sup>2</sup> ) <sup>d</sup>
		Lower	Upper			
N1	687.03	39.36	687.03	1.588±0.60	-4.42±1.95	0.41
N2	1474.86	1087.44	1709.49	1.942±0.57	-6.152±1.84	1.83
N3	981.61	99.52	1321.13	1.404±0.57	-4.20±1.85	0.27
N4	1319.49	685.56	1588.39	1.629±0.57	-5.08±1.83	0.03
N5	999.61	257.19	1306.04	1.596±0.58	-4.79±1.87	0.78
Ridomil gold	204.02	138.44	680.25	0.976±0.31	-2.26±0.62	0.58

<sup>a</sup>The concentration causing 50% mycelial growth inhibition; <sup>b</sup>Slope of the concentration-inhibition regression line ± standard error; <sup>c</sup>Intercept of the regression line ± standard error; <sup>d</sup>Chi square value; Green *P. peruviana* (N1); Red *P. peruviana* (N2); leaves of *P. peruviana* (N3); *S. nigrum* (N4) and *M. oliefera* (N5)

Reports on the mechanism of inhibitory action of silver ions on microorganisms have shown that upon treatment with Ag<sup>+</sup>, DNA loses its ability to replicate resulting in inactivated expression of ribosomal subunit proteins, as well as certain other cellular proteins and enzymes essential to ATP production [35]. It has also been hypothesized that Ag<sup>+</sup> primarily affects the function of membrane-bound enzymes, such as those in the respiratory chain [36].

#### 4. CONCLUSION

The silver nanoparticles have been formed by *P. peruviana*; *S. nigrum* and *M. oliefera* extracts, which is an efficient, eco-friendly and economical process. FT-IR spectrophotometer, XRD, SEM and TEM techniques have confirmed the reduction of silver nitrate to silver nanoparticles. The zones of inhibition were formed in the antimicrobial screening test showed that the Ag NPs synthesized in this process has the efficient antimicrobial activity against the tested pathogenic bacteria and fungi. The biologically synthesized silver nanoparticles could be of immense use in agriculture field for their efficient antimicrobial function. Nanoparticles may be particularly effective delivery systems for plant extracts due to their ability to facilitate antimicrobial application and increase antimicrobial efficacy.

#### COMPETING INTERESTS

Authors have declared that no competing interests exist.

#### REFERENCES

1. Douches DS, Jastrzebski K, Maas D, Chase RW. Assessment of potato

- breeding over the past century. *Crop Sci.* 1996;36:1544-1552.
- Czajkowski R, Pérombelon MCM, van Veen JA, van der Wolf JM. Control of blackleg and tuber soft rot of potato caused by *Pectobacterium* and *Dickeya* species: A review. *Plant Pathol.* 2011; 60:999–1013.
  - Haverkort AJ. Ecology of potato cropping system in relation to latitude and altitude. *Agric. Systems.* 1990;32(3):251-272.
  - Rashid A, Fahad MAB, Khan MA, Mateen A, Farooq M, Ashraf M, Ahmad F, Ahmad M. Incidence of potato blackleg caused by *Pectobacterium atrosepticum* in district Chiniot and its management through bio-products. *African J. Agricultural Res.* 2012;7:6035-6048.
  - Belosokhov AF, Belov GL, Chudinova EM, Kokaeva LY, ELansky SN. *Alternaria spp.* and *Colletotrichum coccodes* in potato leaves with early blight symptoms. *PAGV – Special Report.* 2017;18:181-190.
  - Aliye N, Fininsa C, Hiskias Y. Evaluation of rhizosphere bacterial antagonists for their potential to bioprotect potato (*Solanum tuberosum*) against bacterial wilt (*Ralstonia solanacearum*). *Biol. Control.* 2008;47:282–288.
  - Leite LN, de Haan EG, Krijger M, Kastelein P, der Zouwen PSV, den Bovenkamp GWV, Tebaldi ND, der Wolf JMV. First report of potato blackleg caused by *Pectobacterium carotovorum* subsp. *Brasiliensis* in the Netherlands. *New Disease Reports.* 2014;29:24.
  - Lo'pez MM, Biosca EG. Potato bacterial wilt management: new prospects for an old problem. In Allen C, Prior P, Hayward C. Bacterial wilt disease and the *Ralstonia solanacearum* species complex. *APS*

- Press, St. Paul, Minnesota, USA. 2004;205-224.
9. Okigbo RN, Ogbonnaya UO. Antifungal effects of two tropical plant leaf extract (*Ocimum gratissimum* and *Aframomum melegueta*) on postharvest yam (*Dioscorea spp.*) rot. African J. Biotechnol. 2006;5(9):727-731.
  10. Shariff N, Sudarshana MS, Umesh S, Hari Prasad P. Antimicrobial activity of *Rauvolfia tetraphylla* and *Physalis minima* leaf and callus extracts. African J. Biotechnol. 2006;5(10):946-950.
  11. Varma J, Dubey NK. Prospective of botanical and microbial products as pesticides of Tomorrow. Current Sci. 1999;76:172-179.
  12. Sastry RK, Rashmi HB, Rao NH. Nanotechnology for enhancing food security in India. Food Policy. 2010;36:391-400.
  13. Patil BM, Hooli AA. Evaluation of antibacterial activities of environmental benign synthesis of silver nanoparticles using the flower extracts of *plumeria albalinn*. J. Nanosci. Nanoengin. Appl. 2013;3:19-33.
  14. Maniatis T, Fritsh EF, Sambrook J. Molecular cloning a laboratory manual. Cold Spring Harbor Laboratory, Cold Spring Harbor, N.Y; 1982.
  15. Kelman A. The relationship of the pathogenicity of *Pseudomonas solanacearum* to colony appearance on a tetrazolium medium. Phytopathol. 1954;44:693-695.
  16. Zhang XY, Yu XX, Yu Z, Xue YF, Qi LP. A simple method based on laboratory inoculum and field inoculum for evaluating potato resistance to black scurf caused by *Rhizoctonia solan*. Breeding Sci. 2014;64:156-163.
  17. Banerjee P, Satapathy M, Mukhopahayay A, Das P. Leaf extract mediated green synthesis of silver nanoparticles from widely available Indian plants: synthesis, characterization, antimicrobial property and toxicity analysis: Bioresources and Bioprocessing. 2014;1:3.
  18. Abbassy MA, Masoud SA, Nassar AMK. *In vitro* antibacterial activity and phytochemical analysis of *Abrus precatorius* linn. Egy. J. Plant Pro. Res. 2016;4(2):1-14.
  19. Badawy MEI, Rabea EI, Taktak NEM. Antimicrobial and inhibitory enzyme activity of N-(benzyl) and quaternary N-(benzyl) chitosan derivatives on plant pathogens. Carbohydr. Polym. 2014;111:670-682.
  20. Finney DJ. Statistical logic in the monitoring of reactions to therapeutic drugs. Methods Inf Med. 1971;10(04):237-245.
  21. Weisbrug WG, Barans SM, Pelletier DA, Lane DJ. 16S ribosomal DNA amplification for phylogenetic study. J. Bacteriol. 1991;173:697-703.
  22. White TJ, Bruns T, Lee S, Taylor JW. Amplification and direct sequencing of fungal ribosomal RNA genes for phylogenetic. In: Innis MA, Gelfand DH, Sninsky JJ, White TJ. editors. PCR protocols: A guide to methods and applications. San Diego: Academic Press, 1990;315-322.
  23. Tamura K, Dudley J, Nei M, Kumar S. MEGA4: Molecular evolutionary genetics analysis (MEGA) Software Version 4.0: Mol. Biol. Evol. 2007;24:1596-1599.
  24. Motyka A, Zoledowska S, Sledz W, Lojkowska E. Molecular methods as tools to control plant diseases caused by *Dickeya* and *Pectobacterium* spp. New Biotechnol. 2017;39:181-189.
  25. Onkendi EM, Moleleki LN. Characterization of *Pectobacterium carotovorum* subsp. *Carotovorum* and *Brasiliense* from diseased potatoes in Kenya. Eur. J. Plant Pathol. 2014;139:557-566.
  26. Jain J, Arora S, Rajwade JM, Omray P, Khandelwal S, Paknikar KM. Silver nanoparticles in therapeutics: Development of an antimicrobial gel formulation for topical use. Mol. Pharma. 2009;6(5):1388-1401.
  27. Song JY, Kim SM. Rapid biological synthesis of silver nanoparticles using plant leaf extracts. Bioprocess Biosyst. Eng. 2009;32:79-84.
  28. Krishnaraj C, Jagan SEG, Selvakumar RP, Kalaichelvan PT, Mohan N. Synthesis of silver nanoparticles using *Acalypha indica* leaf extracts and its antibacterial activity against water borne pathogens. Colloids and Surfaces B: Biointerfaces. 2010;76:50-56.
  29. Ali DM, Thajuddin N, Jeganathan K. Plant extract mediated synthesis of silver and gold nanoparticles and its antibacterial activity against clinically isolated pathogens. Colloids and Surfaces B: Biointerfaces. 2011;85:360-365.
  30. Bar H, Bhui DK, Sahoo GP, Sarkar P, De SP, Misra A. Green synthesis of silver

- nanoparticles using latex of *Jatropha curcas*. *Colloids and Surfaces A. Physicochem. Eng. Aspects*. 2009;339:134-139.
31. Veerasamy R, Xin TZ, Gunasagaran S, Xiang TFW, Yang EFC, Jeyakumar N, Dhanaraj SA. Biosynthesis of silver nanoparticles using mangosteen leaf extract and evaluation of their antimicrobial activities. *J. Saudi Chem. Soc.* 2011;2(15): 113-120.
32. Sambhy V, MacBride MM, Peterson BR, Sen A. Silver bromide nanoparticle/polymer composites: Dual action tunable antimicrobial materials. *J. Am. Chem. Soc.* 2006;128(30):9798-9808.
33. Krishnaraj C, Ramachandran R, Mohan K, Kalaichelvan PT. Optimization for rapid synthesis of silver nanoparticles and its effect on phytopathogenic fungi. *Spectrochimica Acta Part A. Mol. Biomol. Spec.* 2012;93:95-99.
34. Narayanan KB, Park HH. Antifungal activity of silver nanoparticles synthesized using turnip leaf extract (*Brassica rapa* L.) against wood rotting pathogens. *Eur. J. Plant Pathol.* 2014;140:185-192.
35. Feng QL, Wu J, Chen GQ, Cui FZ, Kim TN, Kim JO. A mechanistic study of the antibacterial effect of silver ions on *Escherichia coli* and *Staphylococcus aureus*. *National Natural Science Foundation of China.* 2000;52:662-668.
36. McDonnell G, Russell AD. Antiseptics and disinfectants: Activity, action, and resistance. *Am. Soc. Microbiol.* 1999;12: 147-179.

© 2019 Samy et al.; This is an Open Access article distributed under the terms of the Creative Commons Attribution License (<http://creativecommons.org/licenses/by/4.0>), which permits unrestricted use, distribution, and reproduction in any medium, provided the original work is properly cited.

*Peer-review history:*  
The peer review history for this paper can be accessed here:  
<http://www.sdiarticle3.com/review-history/46186>